

Article

Experimental Investigation of the Desalination Process for Direct Contact Membrane Distillation Using Plate and Frame Membrane Module

Yukang Zhou ¹, Long Chen ², Mengtao Huang ¹, Weilian Hu ¹, Guicai Chen ^{1,*} and Binxin Wu ^{3,*}

¹ School of Biological & Chemical Engineering, Zhejiang University of Science and Technology, Hangzhou 310023, China; 212103817036@zust.edu.cn (Y.Z.); 222203855043@zust.edu.cn (M.H.); 105013@zust.edu.cn (W.H.)

² College of Mechanical and Electrical Engineering, Changchun University of Science and Technology, Changchun 130013, China; chenlong1988@zju.edu.cn

³ College of Biosystems Engineering and Food Science, Zhejiang University, Hangzhou 310058, China

* Correspondence: 119032@zust.edu.cn (G.C.); bwu66@zju.edu.cn (B.W.)

Abstract: Through experiments, the effect of membrane material selection and operating conditions on permeate fluxes in direct contact membrane distillation (DCMD) desalination was investigated. The experiment used a plate and frame membrane module, and with nine different hydrophobic porous membranes, a comparative analysis of the desalination performance of 3 wt% NaCl solution was performed. The results of this experiment were compared to find out the effect of different materials, pore sizes and membrane thicknesses on the permeate flux under same operating conditions. Further, a three-factor, three-level orthogonal experiment was designed. The effects of hot-side temperature, hot-side inlet flow and cold-side inlet flow on the permeate flux of PTFE membranes with a pore size of 0.22 μm were investigated when the temperature on the cold side was set at 20 °C. The results showed that in the DCMD experiments, both PTFE and PVDF membranes performed well, and that hot-side inlet temperatures and cold-side inlet flow rates had significant effects on the permeate flux.

Keywords: direct contact membrane distillation; desalination; plate and frame membrane module; permeate flux



Citation: Zhou, Y.; Chen, L.; Huang, M.; Hu, W.; Chen, G.; Wu, B. Experimental Investigation of the Desalination Process for Direct Contact Membrane Distillation Using Plate and Frame Membrane Module. *Appl. Sci.* **2023**, *13*, 9439. <https://doi.org/10.3390/app13169439>

Academic Editors: Negisa Darajeh and Shahabaldin Rezania

Received: 7 July 2023

Revised: 15 August 2023

Accepted: 18 August 2023

Published: 21 August 2023



Copyright: © 2023 by the authors. Licensee MDPI, Basel, Switzerland. This article is an open access article distributed under the terms and conditions of the Creative Commons Attribution (CC BY) license (<https://creativecommons.org/licenses/by/4.0/>).

1. Introduction

Water resource depletion is a widespread issue on a global scale. With the growth of the global economy and the increase in population, this problem has become increasingly prominent [1,2]. At present, the best solution to the lack of water resources is conservation while also developing and utilizing techniques to treat water of poor quality. Figuring out how to solve the problems of seawater desalination and sewage treatment cost effectively and in an energy-efficient way has become the key to solving the problem of water shortage [3,4]. Membrane processes are now important in water treatment in many countries, because membrane separation has more advantages than thermal technology [5]. In particular, this includes avoiding expensive and inefficient heat, and a reduction in environmental problems associated with fuel combustion, thereby reducing production costs. Nevertheless, well-known membrane separation techniques, such as reverse osmosis (RO) [6], have been proven to be unsuitable for current need, which include, for example, the connection between membrane permeability and selectivity, while employing membrane technology for specific purposes [7,8]. For example, for the desalination of high salt feed liquid, high level pre-treatment requirements for raw materials, and higher level of membrane contamination resistance, many membranes are ineffective at removing newly developed pollutants and small-molecule pollutants from water [9,10] since membranes only have the ability to concentrate these contaminants and not completely eliminate them.

Thus, researchers attempted to combine membrane separation technology with the aid of thermal distillation technology to integrate the relative merits of two approaches, namely membrane distillation (MD) [11,12].

MD is a separation technique that relies on heat. The temperature difference between the membrane's two sides acts as the engine for heat transfer, which leads to a vapor pressure difference [13,14]; this causes vapor to go through the membrane pores, inside the membrane module, and the condensation to pure water occurs at the cool liquid/gas interface [15]. On feeds that include volatility solutes [16], when these solutes' boiling points are lower than those of water, they will pass through the membrane so as to separate the raw material liquid. Due of MD's non-isothermal properties, a film that is hydrophobic will not be soaked by water; therefore, membrane contamination is not easy to occur. When compared to conventional membrane methods like RO [17,18], it has a higher interception rate for solutes, and is unaffected by high salt solutions and high permeate pressure. Furthermore, lower operating levels of pressure and temperature are possible for MD [19,20] because the membrane barrier only necessitates a narrower vapor space. It works well with green power sources or thermal waste sources [20,21]. Additionally, because of its less complex configuration, it is becoming a practical separation process that can be used in ocean water and brackish water desalination, in the preparation of ultrapure water [22], chemical material recovery and concentration, watery solutions' volatile solutes' removal and recovery, in juice from fruit and liquid food concentration, in cleaning up sewage, and in other fields [23]. Especially in the treatment of wastewater, membrane distillation can operate at extremely high concentrations, even to saturation, compared to other membrane processes [24,25].

MD technologies include DCMD (Direct Contact Membrane Distillation) [26], where the membrane on the permeate side and the liquid on the cold side are in direct contact; AGMD (Air Gap Membrane Distillation) [27,28], where, on the permeate side, the air gap serves as a condensing surface; SGMD (Sweeping Gas Membrane Distillation), wherein the evaporation of less volatile molecules is aided when the gas is driven through a gap on the permeable side; and VMD (Vacuum Membrane Distillation), where vacuum has an impact on the gap channel's structure [29], owing to DCMD's lack of a need for an additional condenser, which has led to it attracting increasing amounts of attention for being better suited to water applications. In terms of MD configuration, DCMD is the most straightforward method as high-permeate flux can be obtained under simple operating circumstances despite the fact that DCMD has a low thermal efficiency, and a low effective drive due to evaporator proximity to condenser surface [30]. AGMD has high heat utilization efficiency and a low permeate flux. Additionally, SGMD has remarkable thermal efficiency; however, achieving a high permeate flux demands a large flow rate of swept gas. VMD has a greater permeate flux and thermal efficiency. As with the DCMD, by raising the temperature of the feed and flow rate, the VMD's efficiency can be enhanced. However, the VMD setup process is quite complex, mainly due to the need for vacuum and an external condenser [31,32]. This is a serious flaw in VMD; because of this drawback, one of the least researched desalination MD configurations is VMD. In addition, compared to DCMD, a higher productivity at cooler temperatures is not constantly ensured by the VMD's configuration complexity. Because of its simple structure, DCMD can be used at low temperatures and its permeate flux is superior to that of VMD [33]. VMD only has advantages when temperatures or flow rates are higher. In addition, unlike DCMD, VMD does not directly control the permeate-side temperature, and vacuum pressure can also only be realized using vacuum pumps. In VMD, due to the application of vacuum, membrane surfaces may also show significant high-pressure changes; ultimately, the membrane may be wetted or become less hydrophobic. Therefore, DCMD is the most suitable choice for desalination research. In the DCMD, on both surfaces of the hydrophobic membrane, the liquid flows with various temperatures [34,35]. As seen in Figure 1, the liquid is in direct contact with the hydrophobic membrane. Liquid on the feed side does not flow across the membrane surface. The driving force is the disparity in vapor pressure brought on by

the temperature disparity, causing the volatile substances in the hot solution on the feed side to undergo a phase transition. The gas phase volatile components enter the permeate side through the membrane pores, and the low temperature solution on the permeate side then condenses the gas phase volatile components passed through the membrane pores to dissolve them in the receiving solution [36].

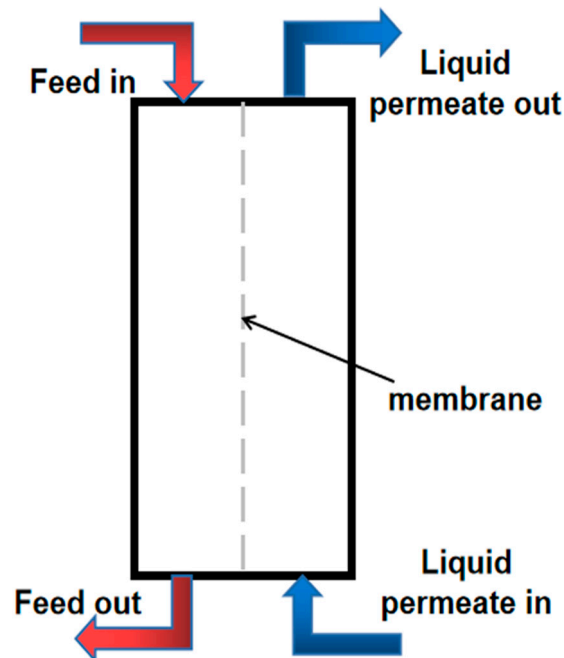


Figure 1. Schematic diagram of DCMD system structure.

Membrane material selection is an important factor in determining DCMD efficiency. Since the variety of DCMD uses, examples include the treatment of factory water, the ground, the ocean, sewage, retrieved water, toxic water, condensation water, and furnace effluent. The total achievement of DCMD processes depends more and more on membranes [37]. Therefore, according to the goal contaminants present in particular uses, the most suitable hydrophobic membrane should be selected accordingly. The most suitable membranes for MD uses include low surface energy, a high degree of porosity (small average size of pore, narrow size of pores spread), and low thermal conductivity. This is because the lower the thermal conductivity of the MD membrane, the less heat can be lost through the membrane.

It is helpful to select appropriate membranes to increase the permeate flux. In their investigation of various membranes, Zhang et al. [38] examined PVDF-MF membranes that were constructed with a nonwoven support layer, PTFE-MF membrane consisting of a nonwoven support layer, and three different kinds of MD membranes manufactured of PTFE, which, though they had varying pore diameters, each featured a support layer made of coarsely structured fabric. The findings demonstrated that, under the same conditions of operation, the permeate flux of PTFE membranes was significantly higher than that of PVDF-MF membranes. Additionally, the findings indicated that raising the rate of feeding and intake temperature would result in an even greater increase in permeate flux, but at extremely high flow rates, the rate of improvement of permeate flux would decrease. According to the type of membrane, DCMDs have different permeate fluxes and conductivities. Test films' LEP, breathability, and CA are able to be compared. Depending on the operating conditions of the test, such as flow rate, temperature and concentration, the device's assembly form may vary. For example, He et al. [17], testing nine commercially available membranes for the production of potable water from brine, found that under all conditions studied, permeate conductivity was always below 8 ms/cm. Nevertheless, the type of saltwater, temperature difference between the two sides, and the ability to

perform of the membrane all affect the quality of the membrane's production. For a PTFE membrane with 0.22 mm pores, an intake water temperature of 60 °C, 20 °C as the permeate temperature, and a flow rate of 0.6 L/min, the permeate flux of seawater desalination is 23.76 L/m²h.

The structure and operating circumstances of the DCMD are the primary determinants of performance. The feed side and permeate side inflows, the heat transfer method, and the material of the membrane module can all significantly affect how productive a DCMD system is. The DCMD system's general efficacy is impacted by the operational parameters chosen. Moreover, considering both the feed and permeate side temperatures is crucial, because increased operating temperatures on the feed side may lead to greater permeate flux when the liquid pressure does not reach the point where it can enter. While higher feed-side temperatures can produce higher permeate flux, at specific operating temperatures, the permeate flux will be determined by factors like flow rate. Mahdi et al. [39] investigated how nine easily accessible PTFE hydrophobic sheet membranes performed on DCMD under different operating parameters, including feed side temperature, feed side flow rate, permeate side flow rate, and feed side density. The experimental study's findings demonstrated that raising the feed side temperature, feed side flow rate and permeate side mold assembly depth could increase the permeate flux. Bahmanyar et al. [32] examined the impact of operating parameters such as feed side temperature, flow rate, and density on permeate flux. After modeling, the problem is solved numerically using mathematical analysis software. The loss of energy via heat conduction and heat exchange was found to have a significant impact. Recently, a more modern technique, response surface methodology, has been used to improve the DCMD process. The mathematical modeling of operational factors impacting DCMD desalination was modeled by Boubakri et al. [40] by applying RSM. A low-pore-size PP membrane was employed. The outcomes demonstrated the model's remarkable coefficient of determination ($R^2 = 0.989$). A vapor pressure differential of 3.55×10^4 Pa was found to be the best working parameter, with a feed flow rate of 73.6 L/h and a permeate flow rate of 17.1 L/h; under these optimal circumstances, the permeate flux was 4.191 L/m²h.

Gunko et al. [41], Pelin et al. [7], and Ramlow et al. [42] explored the factors affecting the permeate flux of DCMD. It was discovered that raising the hot-side temperature, lowering the cold-side temperature, and raising the cold-side flow rate might raise the permeate flux. Ni et al. [43] and Ali et al. [44] looked into how feed temperature, rate affected temperature polarization. It was shown that the temperature polarization rises with increasing feed temperature and decreasing feed and permeate rates. At very low flow rates, the conduction resistance of the membrane dominates, limiting the heat transmission at the membrane contact, which has an impact on the efficiency of the process. Chen et al. [45] and Banat et al. [46] investigated the effect of flow rate on permeate flux on the permeate side, and discovered that increasing the flow rate could increase the heat transfer coefficient and decrease the thermal boundary layer, resulting in a decrease in temperature polarization coefficient. It was indicated that the effect of the feed side was greater than the permeate side in terms of flow rate. For membrane distillation, growing the flow rate of the feed increases the permeate flux but also increases the possibility of membrane wetting. Furthermore, the rise in flow rate may increase the energy consumption of the liquid transport system and the operating cost. Therefore, it is necessary to select the appropriate flow rate to optimize the whole membrane distillation system.

Temperature has also been shown by Manawi et al. [47] to be a crucial operational component that must be carefully taken into account when designing a DCMD process. To calculate the temperature polarization coefficient on the DCMD membrane, a DCMD model was created. Under various operating circumstances, localized permeate fluxes were obtained. When the flow rate was 3 L/min, the feed temperature was 60 °C, and the permeation temperature was 20 °C, it was discovered that the temperature polarization coefficient was at its highest, 0.8. When the feed temperature is 70 °C and the permeate side temperature is 30 °C, at a flow rate of 1.5 L/min, the temperature polarization coefficient

cient is 0.66. However, when other conditions remain unchanged, the temperature of the permeate side increased to 70 °C, and the temperature polarization coefficient reduced to 0.47. It has been demonstrated that the temperature polarization coefficient in DCMD is substantially determined by the internal coefficient of mass transfer of the membranes used. Additionally, Singh [25] noted that a key factor affecting DCMD performance is the membrane material's thermal conductivity. While this was going on, Su et al. [48] carried out experimental and theoretical research to look into the impact of hydrophobic hollow fiber membranes' thermal conductivity on permeate flux. When the feed temperature is 80 °C and the distillate temperature is 20 °C, the hydrophilic layer's thermal conductivity ranges from 0.2 to 1.4 W/mK, and vapor flux increases significantly from 31.4 to 78.5 kg/m²h. Embedding MWCNTs containing graphite particles into the hydrophilic layer of hollow fibers increases its thermal conductivity. With the addition of MWCNTs, the thermal conductivity is twice as high as that before it was added. The obtained thermal conductivity is still rather modest; it was found that by maintaining the distillate and feed temperatures at 15 °C and 80 °C, the thermal conductivity enhanced with the inclusion of nanomaterials, causing a considerable shift in steam vapor flux to 1.6 times the initial steam vapor flux of 40 kg/m²h.

Because the productiveness of the DCMD process is impacted by many operational parameters, researchers are also working on the sensitivity of DCMD productivity to different parameters. To identify the most crucial operating factors, Hayer et al. [49] also carried out a theoretical investigation on the sensitivity of DCMD to different factors using the simulate approach. Using the overall sensitivity evaluation technique, the impacts of various factors on permeate flux and temperature polarization coefficient were quantified. The findings indicate that feed temperature and membrane thickness are crucial design factors in DCMD. Therefore, the selection of operating conditions for DCMD not only has a direct impact on productivity, it also indirectly affects production costs. For, if one seeks only the incremental increase from a single factor, but not considering the whole, increasing the feed temperature can increase permeate flux. However, at this time there is no corresponding increase in the efficiency of heat utilization. Increased energy consumption without improving productivity will lead to cost of production increases, which make this approach not conducive to the development and practical application of membrane distillation.

Based on the above research, this paper conducts a continuous analysis from the selection of hydrophobic porous membrane materials to the study of optimal operating conditions, supplying a guide for the DCMD desalination process's optimization.

2. Materials and Methods

2.1. The Evaluation Index of Membrane Distillation

Permeate Flux

Permeate flux is the mass of pure water produced per unit membrane area and per unit time, which can be calculated as follows:

$$J = \frac{m}{tA} \quad (1)$$

where J is the permeate flux, kg/m²·h; m is the electronic balance reading, g; A is the effective evaporation membrane area, m²; and t is the recording time, s.

2.2. Experimental Materials and Equipment

As shown in Figure 2, the PTFE, PVDF, and PP flat sheet hydrophobic porous membranes were used in the experiments. Figure 3 shows the DCMD system. Figure 4 shows images captured via SEM (scanning electron microscopy) of membrane samples. Tables 1 and 2 show the equipment and the physical property parameters of selected hydrophobic porous membranes, respectively.

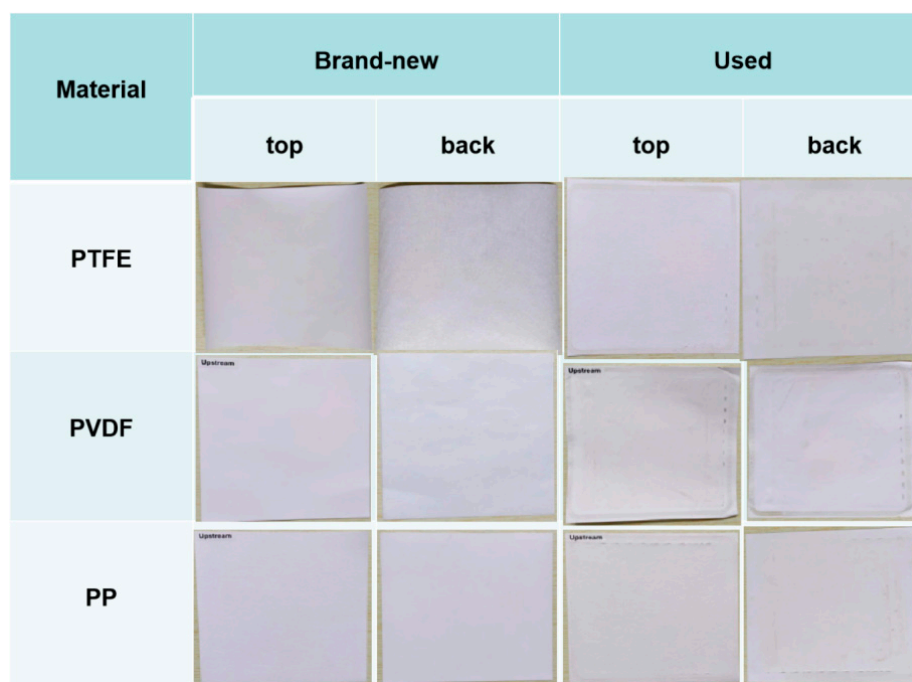


Figure 2. The three different hydrophobic porous membranes used in the experiments.

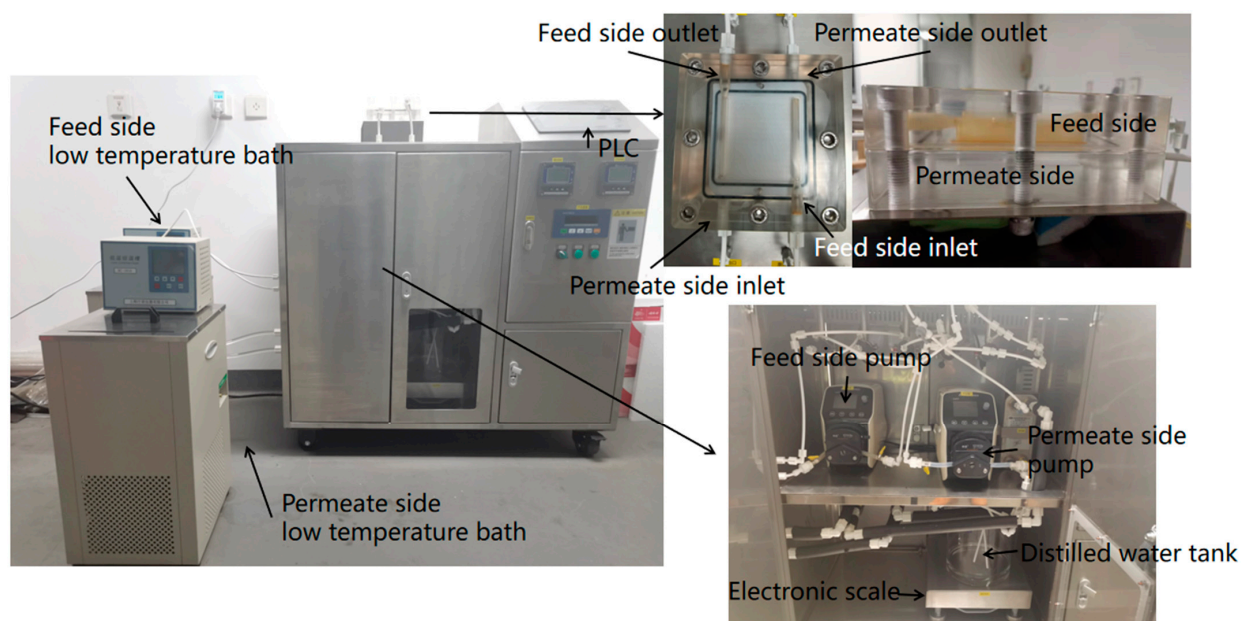


Figure 3. Direct contact membrane distillation equipment.

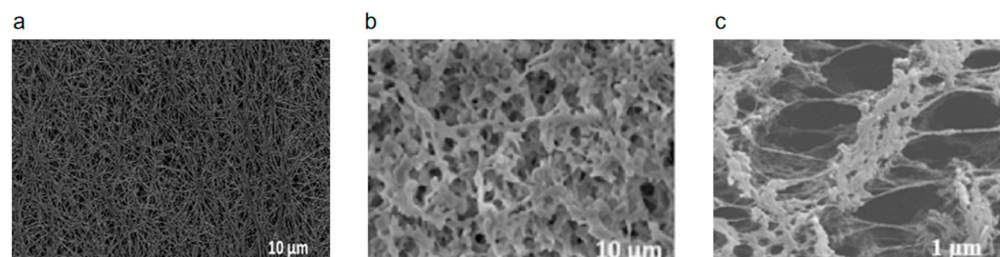


Figure 4. Images captured via SEM (scanning electron microscopy) of membrane samples' inside surfaces (a) PTFE [50], (b) PVDF [50], (c) PP [51].

Table 1. DCMD system components.

Equipment	Equipment Model	Manufacturers
Membrane	MFPT-2213	Hangzhou Cobalt Filter Material Co., Hangzhou China.
Membrane Components		Xiamen Guochu Co., Xiamen China.
Pump	YZ-1515X	Lange Constant Flow Pump Co., Baoding China.
Constant Temperature Tank	DC-1010	Xiamen Guochu Co., Xiamen China.
Temperature and conductivity sensors	EC-4110	Suntex Instruments Co., Taiwan China.
Electronic scale	XH3180-K	Xinhen Instruments Co., Shanghai China.

Table 2. Physical property parameters of the selected hydrophobic porous membranes.

	Thickness (μm)	Pore Size (μm)	Thermal Conductivity ($\text{W}\cdot\text{m}^{-1}\cdot\text{K}^{-1}$)	Porosity %	Contact Angle ($^{\circ}$) [5,17,52]
PTFE	205	0.22	0.2651	53.75	140 ± 3
	185	0.45	0.2651	46.77	140 ± 3
	168	1	0.2651	53.12	140 ± 3
PP	177	0.22	0.13	55.22	148.1
	193	0.45	0.13	37.73	148.1
	228	1	0.13	55.89	148.1
PVDF	150	0.22	0.22	85	120 ± 10
	125	0.45	0.22	90	120 ± 10
	100	1	0.22	90	120 ± 10

(1) Membrane module

The membrane module employed in this work was composed of one upper and one lower cover plate (Polymeric Methyl Methacrylate Material), a membrane, a spacer (Acrylonitrile Butadiene Styrene Material), and two gaskets (Natural Rubber Material). The membrane and the spacer were overlapped. This module has a surface area of 0.03 m^2 , and the feed and coolant/permeate chambers both have a surface area of 0.01 m^2 . The sealing gasket was placed between the membrane and the cover plates. Figure 5 shows the membrane module structure.

(2) Feed side (hot-side) pump

The feed side pump was used to provide enough pressure for the raw solution in the thermostatic bath to enter the membrane module. The adjustment range of flow rate is 0–1000 mL/min, and it can achieve infinitely precise adjustment, with a pipe wall thickness of 1.5 mm.

(3) Constant Temperature Tank

The constant temperature tank is divided into heating constant temperature tank and cooling constant temperature tank; the temperature adjustment range is 0–100 $^{\circ}\text{C}$, the precision is 0.01 $^{\circ}\text{C}$, and the maximum that can be heated or condensed is 10 L of liquid. The heating constant temperature tank is used to heat the material liquid, and the cooling constant temperature tank provides condensation on the cold water side.

(4) Electronic scale

The function of the electronic balance is to accurately measure the weight of water produced. The measurable range is from 0 to 2000 g, with an accuracy of 0.1 g.

(5) Permeate side (cold-side) pump

The permeate side pump was used to cool the water in the cryogenic chiller to a set temperature, providing sufficient pressure to enter the membrane module. The adjustment range of flow rate is 0–1000 mL/min, and it can achieve infinitely precise adjustment, with a pipe wall thickness of 1.5 mm.

(6) Temperature and conductivity sensors

The temperature and conductivity sensors were used to detect the temperature and conductivity of the hot and cold sides in actual time. The temperature detection range of the hot side is from 0 to 100 °C and the conductivity detection range is from 0 to 199 ms/cm, with an accuracy of 0.01 ms/cm. The temperature detection range of the cold side is from 0 to 100 °C and the conductivity detection range is from 0 to 2000 μ s/cm, with an accuracy of 0.01 μ s/cm.

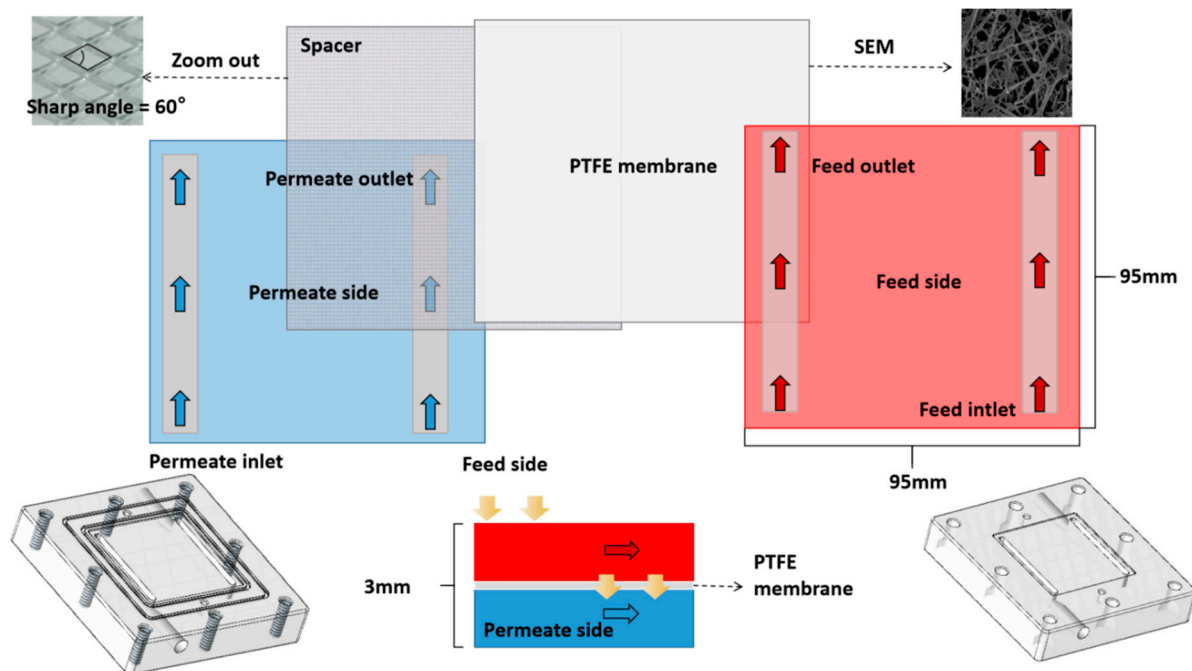


Figure 5. Membrane module structure.

The experimental steps were as follows:

Firstly, each group of test lasted for 3 h, and after the system was stabilized, the data were recorded every 15 min, and a total of 12 groups of data were recorded in each test;

Then, the stable data of each group of tests were arithmetically averaged to find the average permeate flux and error calculations were performed.

The aim of this article is to determine the optimal time for membrane performance without considering pollution. In subsequent studies, the situation of membrane fouling will be studied separately.

3. Results and Discussion

3.1. Effect of Membrane Materials on the Permeate Flux of the DCMD Process

The experimental comparison of different membrane materials was conducted under the operations of 50 °C hot-side inlet temperature, 20 °C cold-side inlet temperature, 500 mL/min hot-side flow rate, 500 mL/min cold-side flow rate, and 3 wt% NaCl (300 g salt mixed with 10 L water) of the solution to be separated. During the experiment, the conductivity of the produced water was controlled below 10. Table 3 shows the experimental results.

The experimental results indicate that both PTFE and PVDF membranes perform well, whereas pp membranes are not recommended. The permeate flux increases as the membrane pore size increases without considering any membrane fouling and scale-up issues. The optimal membrane pore size in this study is 1.0 μ m.

Table 3. The performance of different membrane materials in DCMD experiments.

Scenario	Pore Size A (μm)	Material B	Average Permeate Flux/J kg/(m ² *h)
1	0.22	PTFE	8.62
2	0.45	PTFE	11.42
3	1.0	PTFE	12.87
4	0.22	PVDF	8.40
5	0.45	PVDF	10.25
6	1.0	PVDF	11.64
7	0.22	PP	2.00
8	0.45	PP	1.16
9	1.0	PP	4.00

As shown in Figure 6a, the total average permeate flux of a PTFE membrane with 1.0 μm pore size is 12.87 kg/(m²*h), which fluctuates up and down from 15 to 60 min of the MD process and then stabilizes after 90 min. The average permeate flux for PTFE membranes with pore sizes of 0.45 μm is 11.42 kg/(m²*h). The total average permeate flux for a PTFE membrane with a pore size of 0.22 μm is 8.62 kg/(m²*h), which increases significantly from 15 to 60 min of the MD process and then fluctuates after the 60 min. The fluctuation of permeate flux is mainly due to the jittering of the experimental water pipe, which causes some experimental errors. For errors, the data use the mean value. The relative error between each set of data and the mean was then calculated. Finally, the error results were all calculated to be within 4%, which is within the allowable error range.

As shown in Figure 6b, the total average permeate flux of a PVDF membrane with a pore size of 1.0 μm is 11.64 kg/(m²*h), with an overall decreasing trend and a significant decrease from 60 to 90 min of the process, and it tends to be stable after 135 min. The total average permeate flux of PVDF membrane with a pore size of 0.45 μm is 10.25 kg/(m²*h), and it fluctuates up and down during the process. The total average value of permeate flux for PVDF membrane with a pore size of 0.22 μm is 8.40 kg/(m²*h), and the average value remains relatively stable.

Figure 6c shows the performance of the PP membranes in the DCMD desalination process. The total average permeate flux of a PP membrane with a pore size of 1.0 μm is 4.00 kg/(m²*h), with an overall increasing trend. The permeate flux increases when the process is running from 30 to 60 min, and it is stable after 135 min. The total average permeate flux of a PP membrane with a pore size of 0.45 μm is 1.16 kg/(m²*h), with an overall decreasing trend. It decreases after 45 min and becomes stable gradually. The total average permeate flux of a PP membrane with a pore size of 0.22 μm is 2.00 kg/(m²*h). The decline from 60 to 75 min is greater than that from 90 to 105 min, and it is stable after 135 min.

Figure 7 illustrates how the performance of the DCMD desalination system is impacted by membrane thickness. Membrane thickness has an inverse relationship with the permeate fluxes of PVDF and PTFE membranes, while the permeate fluxes of PP membranes change insignificantly with the increase in thickness and remain at a low permeate flux.

Figure 8 shows the effect of membrane pore size on the desalination performance of hydrophobic porous membranes with pore sizes of 0.22 μm , 0.45 μm , and 1.0 μm . It can be seen that the differences between the permeate fluxes of PTFE and PVDF membranes are small, while PP membrane's permeate flux is significantly lower than that of the others.

This situation arises because the PVDF membrane has moderate thermal stability and a surface energy of 3.03×10^{-2} N/m. The thermal stability of PP membrane at high temperatures is average, with a surface energy of 3.0×10^{-3} N/m, with lower membrane performance. Additionally, PTFE membrane has good thermal stability, with the lowest surface energy of 9.0×10^{-3} – 2.0×10^{-2} N/m [53]. In addition, it has high vapor permeability and high moisture resistance. Therefore, the highest permeate flux is produced by PTFE membranes with low surface energy, high porosity (narrow size of pores dispersion, small average size of pores), and low thermal conductivity.

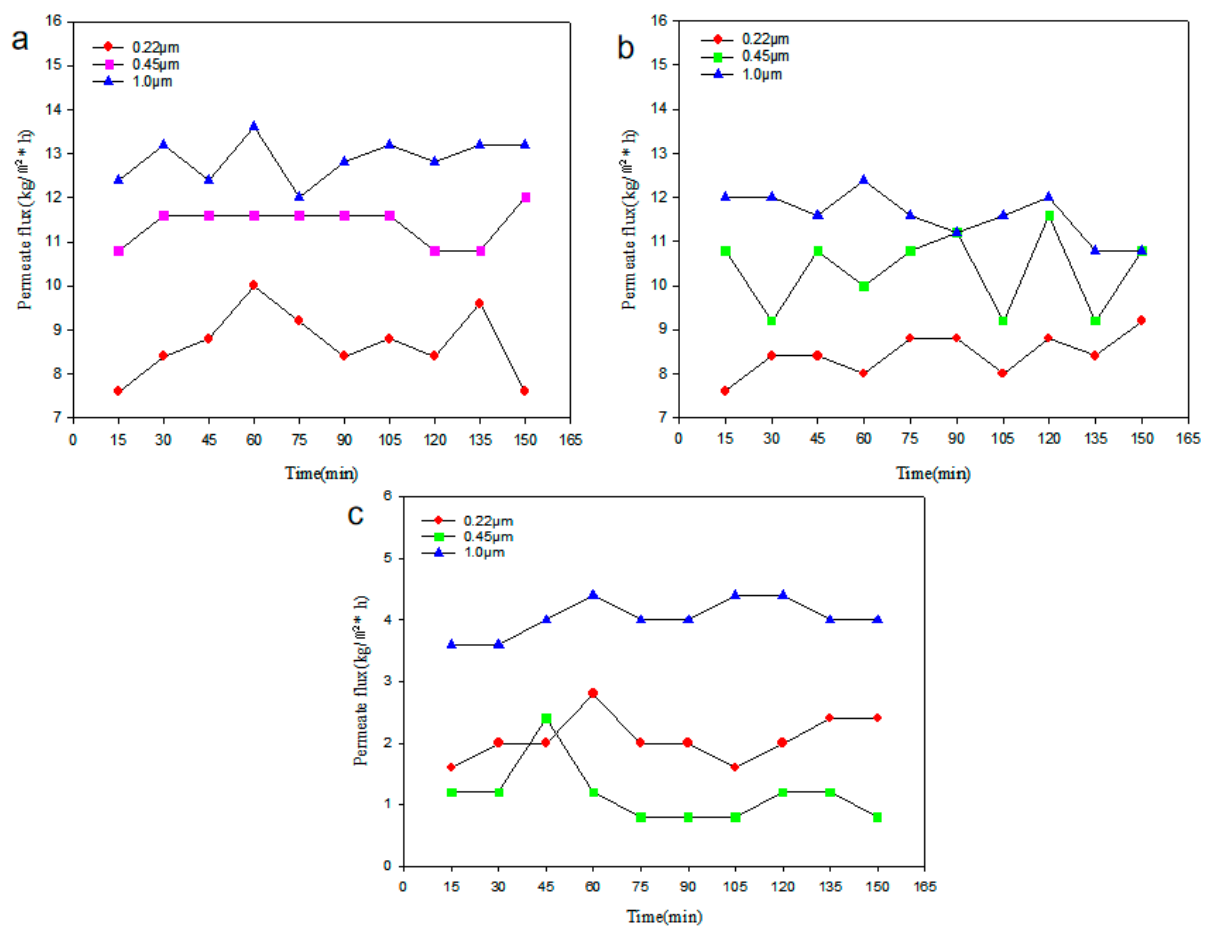


Figure 6. Comparison of membrane permeate fluxes with different pore sizes (a) PTFE, (b) PVDF, (c) PP.

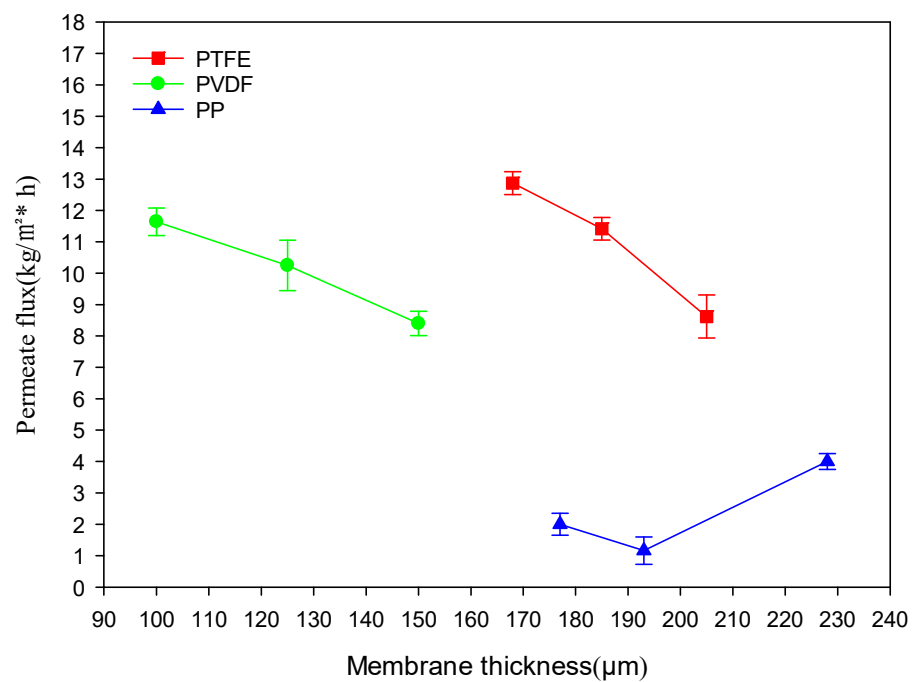


Figure 7. Relationship between membrane thickness and permeate flux for different membrane materials.

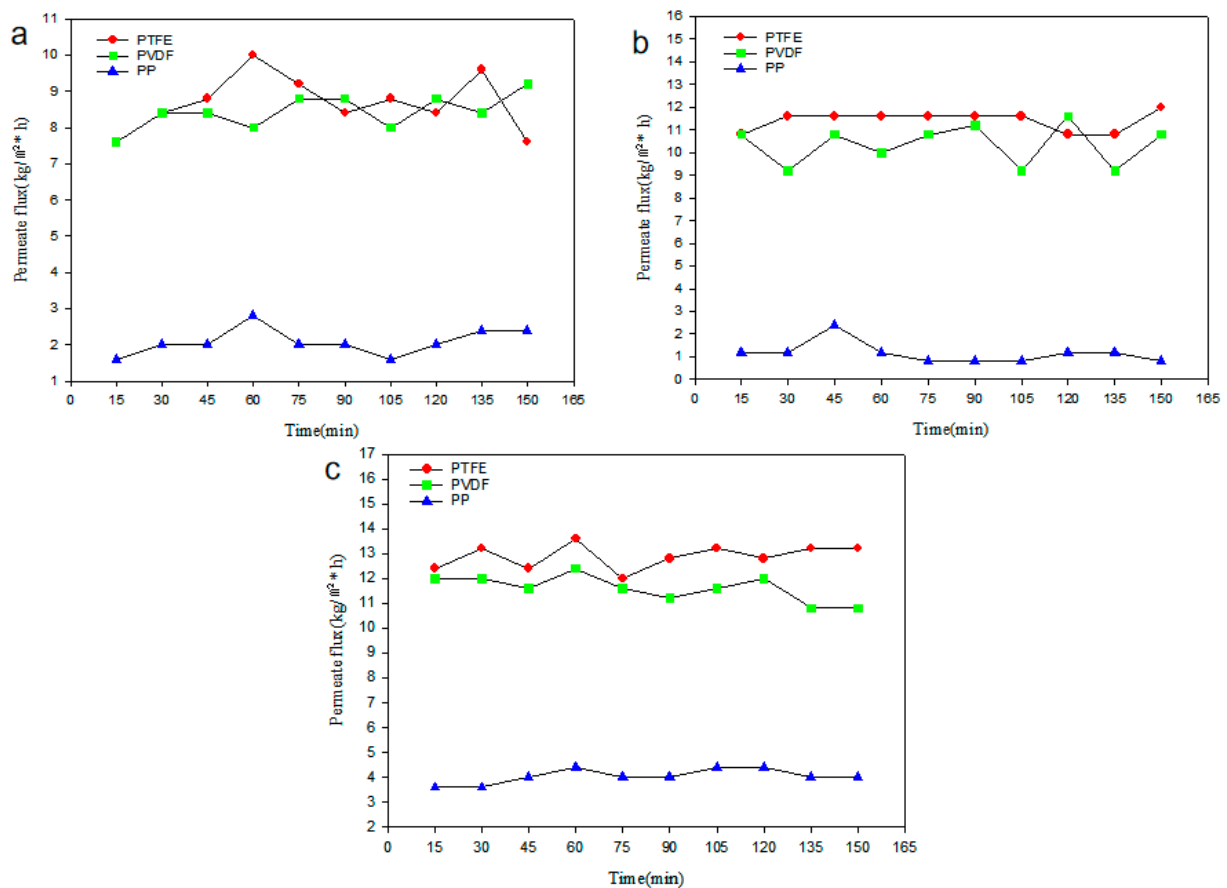


Figure 8. Comparison of membrane permeate flux of different membrane materials. (a) 0.22 μm , (b) 0.45 μm , (c) 1.0 μm .

3.2. The Effect of Operational Conditions on the DCMMD Process

An orthogonal experiment was designed to study the relationships among the temperature of the hot side, the flow rate of the hot side, the flow rate of the cold side and the permeate flux. Table 4 shows the factors in the experiment. The solution to be separated was 3 wt% NaCl solution. PTFE membranes with a pore size of 0.22 μm were selected. The cold side's temperature remained constant at 20 $^{\circ}\text{C}$. The experiment was conducted with three different hot-side inlet temperatures (60, 70, and 80 $^{\circ}\text{C}$) and three different inlet flow rates (600, 800, and 1000 mL/min). During the experiment, the conductivity of the produced water was controlled below 10. Table 5 shows the experimental results, from which the optimal combination $A_3B_1C_3$ can be obtained.

Table 4. The factors in the orthogonal experiment.

Level	Hot-Side Temperature A ($^{\circ}\text{C}$)	Hot-Side Inlet Flow Rate B (mL/min)	Cold-Side Inlet Flow Rate C (mL/min)
1	60	600	600
2	70	800	800
3	80	1000	1000

Table 5. The orthogonal experimental results.

Scenario	Hot-Side Temperature A (°C)	Hot-Side Inlet Flow Rate B (mL/min)	Cold-Side Inlet Flow Rate C (mL/min)	Average Permeate flux/J kg/(m ² *h)	Standard Deviation
1	60	600	600	15.4	1.07
2	60	800	800	16.1	0.85
3	60	1000	1000	17.4	1.39
4	70	600	800	23.8	1.17
5	70	800	1000	25.2	1.03
6	70	1000	600	23.6	1.26
7	80	600	1000	35.8	1.15
8	80	800	600	30.8	0.97
9	80	1000	800	31.7	1.40
yl1	48.9	75.0	69.8	ΣJ = 219.8	
yl2	72.6	72.1	72.8		
yl3	98.3	72.7	78.4		
ȳ _{j1}	16.30	25.00	23.27		
ȳ _{j2}	24.20	24.03	24.27		
ȳ _{j3}	32.77	24.23	26.13		
R _j	16.47	0.77	2.86		
Excellent level	A ₃	B ₁	C ₃		
Primary and secondary factors	A	C	B		
Optimal combination		A ₃ B ₁ C ₃			

4. Conclusions

The following are the findings from the experimental study of the DCMD desalination process:

- (1) PTFE and PVDF membranes are the best choice of membrane materials for membrane distillation, whereas pp membranes are not recommended. The permeate fluxes of PVDF and PTFE membranes are very close when their pore sizes are 1.0 μm.
- (2) Without considering the membrane fouling and scale-up issues caused by long-time desalination processes, the permeate flux of PTFE and PVDF membrane increases with the increase in the pore size. In contrast, the permeate flux of pp membranes does not vary significantly with pore size. Additionally, in this study, $J_{pvd1.0} = 1.136J_{pvd0.45} = 1.386J_{pvd0.22}$, $J_{ptfe1.0} = 1.267J_{ptfe0.45} = 1.377J_{ptfe0.22}$.
- (3) Under operating conditions of constant inlet flow on the hot and cold sides, increasing the hot-side temperature and decreasing the cold-side temperature facilitates the increase in permeate flux in membrane distillation systems. Moreover, the hot-side temperature and cold-side inlet flow rate have a greater influence on improving the permeate flux, and the optimal combination is A₃B₁C₃ in this experiment.

Author Contributions: Writing—original draft, Y.Z.; writing—review and editing, L.C.; Conceptualization, M.H. and W.H.; Resources, G.C. and B.W. All authors have read and agreed to the published version of the manuscript.

Funding: This research was funded by Zhejiang Provincial Key R&D Program of China (2022C02013).

Institutional Review Board Statement: Not applicable.

Informed Consent Statement: Not applicable.

Data Availability Statement: Not applicable.

Conflicts of Interest: The authors declare no conflict of interest.

References

- Chen, L.; Wu, B. Research Progress in Computational Fluid Dynamics Simulations of Membrane Distillation Processes: A Review. *Membranes* **2021**, *11*, 513. [\[CrossRef\]](#) [\[PubMed\]](#)
- Drioli, E.; Ali, A.; Macedonio, F. Membrane distillation: Recent developments and perspectives. *Desalination* **2015**, *356*, 56–84. [\[CrossRef\]](#)
- Khan, A.; Yadav, S.; Ibrar, I.; Al Juboori, R.A.; Razzak, S.A.; Deka, P.; Subbiah, S.; Shah, S. Fouling and Performance Investigation of Membrane Distillation at Elevated Recoveries for Seawater Desalination and Wastewater Reclamation. *Membranes* **2022**, *12*, 951. [\[CrossRef\]](#) [\[PubMed\]](#)
- Khayet, M. Membranes and theoretical modeling of membrane distillation: A review. *Adv. Colloid Interface Sci.* **2011**, *164*, 56–88. [\[CrossRef\]](#) [\[PubMed\]](#)
- Eleiwi, F.; Ghaffour, N.; Alsaadi, A.S.; Francis, L.; Laleg-Kirati, T.M. Dynamic modeling and experimental validation for direct contact membrane distillation (DCMD) process. *Desalination* **2016**, *384*, 1–11. [\[CrossRef\]](#)
- Li, Z.; Peng, Y.; Dong, Y.; Fan, H.; Chen, P.; Qiu, L.; Jiang, Q. Effects of thermal efficiency in DCMD and the preparation of membranes with low thermal conductivity. *Appl. Surf. Sci.* **2014**, *317*, 338–349. [\[CrossRef\]](#)
- Yazgan-Birgi, P.; Ali, M.I.H.; Arafat, H.A. Comparative performance assessment of flat sheet and hollow fiber DCMD processes using CFD modeling. *Sep. Purif. Technol.* **2019**, *212*, 709–722. [\[CrossRef\]](#)
- Abu-Zeid MA, E.R.; Zhang, Y.; Dong, H.; Zhang, L.; Chen, H.L.; Hou, L. A comprehensive review of vacuum membrane distillation technique. *Desalination* **2015**, *356*, 1–14. [\[CrossRef\]](#)
- Andrés-Mañas, J.A.; Ruiz-Aguirre, A.; Acién, F.G.; Zaragoza, G. Assessment of a pilot system for seawater desalination based on vacuum multi-effect membrane distillation with enhanced heat recovery. *Desalination* **2018**, *443*, 110–121. [\[CrossRef\]](#)
- Andrjesdóttir, Ó.; Ong, C.L.; Nabavi, M.; Paredes, S.; Khalil, A.S.G.; Michel, B.; Poulikakos, D. An experimentally optimized model for heat and mass transfer in direct contact membrane distillation. *Int. J. Heat Mass Transf.* **2013**, *66*, 855–867. [\[CrossRef\]](#)
- Camacho, L.M.; Dumée, L.; Zhang, J.; Li, J.D.; Duke, M.; Gomez, J.; Gray, S. Advances in membrane distillation for water desalination and purification applications. *Water* **2013**, *5*, 94–196. [\[CrossRef\]](#)
- Elmarghany, M.R.; El-Shazly, A.H.; Salem, M.S.; Sabry, M.N.; Nady, N. Thermal analysis evaluation of direct contact membrane distillation system. *Case Stud. Therm. Eng.* **2019**, *13*, 100377. [\[CrossRef\]](#)
- Ashoor, B.B.; Mansour, S.; Giwa, A.; Dufour, V.; Hasan, S.W. Principles and applications of direct contact membrane distillation (DCMD): A comprehensive review. *Desalination* **2016**, *398*, 222–246. [\[CrossRef\]](#)
- Ge, J.; Peng, Y.; Li, Z.; Chen, P.; Wang, S. Membrane fouling and wetting in a DCMD process for RO brine concentration. *Desalination* **2014**, *344*, 97–107. [\[CrossRef\]](#)
- Manawi, Y.M.; Khraisheh, M.; Fard, A.K.; Benyahia, F.; Adham, S. Effect of operational parameters on distillate flux in direct contact membrane distillation (DCMD): Comparison between experimental and model predicted performance. *Desalination* **2014**, *336*, 110–120. [\[CrossRef\]](#)
- Francis, L.; Ghaffour, N.E.; Alsaadi, A.S.; Nunes, S.P.; Amy, G.L. Performance evaluation of the DCMD desalination process under bench scale and large scale module operating conditions. *J. Membr. Sci.* **2014**, *455*, 103–112. [\[CrossRef\]](#)
- He, K.; Hwang, H.J.; Woo, M.W.; Moon, I.S. Production of drinking water from saline water by direct contact membrane distillation (DCMD). *J. Ind. Eng. Chem.* **2011**, *17*, 41–48. [\[CrossRef\]](#)
- Baig, U.; Faizan, M.; Waheed, A. A review on super-wettable porous membranes and materials based on bio-polymeric chitosan for oil-water separation. *Adv. Colloid Interface Sci.* **2022**, *303*, 102635. [\[CrossRef\]](#)
- Baig, U.; Waheed, A.; Dastageer, M.A. Facile fabrication of silicon carbide decorated ceramic membrane, engineered with selective surface wettability for highly efficient separation of oil-in-water emulsions. *J. Environ. Chem. Eng.* **2023**, *11*, 109357. [\[CrossRef\]](#)
- Okati, V.; Moghadam, A.J.; Farzaneh-Gord, M.; Moein-Jahromi, M. Thermo-economical and environmental analyses of a Direct Contact Membrane Distillation (DCMD) performance. *J. Clean. Prod.* **2022**, *340*, 130613. [\[CrossRef\]](#)
- Criscuoli, A. Experimental investigation of the thermal performance of new flat membrane module designs for membrane distillation. *Int. Commun. Heat Mass Transf.* **2019**, *103*, 83–89. [\[CrossRef\]](#)
- Okabe, K. Experimental simulation of membrane module performance in direct contact membrane distillation. *Int. J. Heat Mass Transf.* **2021**, *172*, 121188. [\[CrossRef\]](#)
- Deshpande, J.; Nithyanandam, K.; Pitchumani, R. Analysis and design of direct contact membrane distillation. *J. Membr. Sci.* **2017**, *523*, 301–316. [\[CrossRef\]](#)
- Boubakri, A.; Hafiane, A.; Bouguecha, S.A.T. Direct contact membrane distillation: Capability to desalt raw water. *Arab. J. Chem.* **2017**, *10*, S3475–S3481. [\[CrossRef\]](#)
- Singh, D.; Sirkar, K.K. Desalination of brine and produced water by direct contact membrane distillation at high temperatures and pressures. *J. Membr. Sci.* **2012**, *389*, 380–388. [\[CrossRef\]](#)
- Ho, C.D.; Huang, C.H.; Tsai, F.C.; Chen, W.T. Performance improvement on distillate flux of countercurrent-flow direct contact membrane distillation systems. *Desalination* **2014**, *338*, 26–32. [\[CrossRef\]](#)
- Deshmukh, A.; Elimelech, M. Understanding the impact of membrane properties and transport phenomena on the energetic performance of membrane distillation desalination. *J. Membr. Sci.* **2017**, *539*, 458–474. [\[CrossRef\]](#)
- Swaminathan, J.; Chung, H.W.; Warsinger, D.M. Simple method for balancing direct contact membrane distillation. *Desalination* **2016**, *383*, 53–59. [\[CrossRef\]](#)

29. Soukane, S.; Naceur, M.W.; Francis, L.; Alsaadi, A.; Ghaffour, N. Effect of feed flow pattern on the distribution of permeate fluxes in desalination by direct contact membrane distillation. *Desalination* **2017**, *418*, 43–59. [\[CrossRef\]](#)
30. Lee, J.G.; Kim, W.S.; Choi, J.S.; Ghaffour, N.; Kim, Y.D. A novel multi-stage direct contact membrane distillation module: Design, experimental and theoretical approaches. *Water Res.* **2016**, *107*, 47–56. [\[CrossRef\]](#)
31. Bouchrit, R.; Boubakri, A.; Hafiane, A.; Bouguecha, S.A.T. Direct contact membrane distillation: Capability to treat hyper-saline solution. *Desalination* **2015**, *376*, 117–129. [\[CrossRef\]](#)
32. Bahmanyar, A.; Asghari, M.; Khoobi, N. Numerical simulation and theoretical study on simultaneously effects of operating parameters in direct contact membrane distillation. *Chem. Eng. Process. Process Intensif.* **2012**, *61*, 42–50. [\[CrossRef\]](#)
33. Liu, Y.J.; Han, J.T.; Wang, Y.S.; Tien-Chien, J. Experimental study on saline solution by direct contact membrane distillation. *CIESC J.* **2018**, *69*, 246–251.
34. Katsandri, A. A theoretical analysis of a spacer filled flat plate membrane distillation modules using CFD: Part II: Temperature polarisation analysis. *Desalination* **2017**, *408*, 166–180. [\[CrossRef\]](#)
35. Khayet, M.; Matsuura, T.; Mengual, J.I.; Qtaishat, M. Design of novel direct contact membrane distillation membranes. *Desalination* **2006**, *192*, 105–111. [\[CrossRef\]](#)
36. Khalifa, A.; Ahmad, H.; Antar, M.; Laoui, T.; Khayet, M. Experimental and theoretical investigations on water desalination using direct contact membrane distillation. *Desalination* **2017**, *404*, 22–34. [\[CrossRef\]](#)
37. El-Bourawi, M.S.; Ding, Z.; Ma, R.; Khayet, M. A framework for better understanding membrane distillation separation process. *J. Membr. Sci.* **2006**, *285*, 4–29. [\[CrossRef\]](#)
38. Zhang, J.; Dow, N.; Duke, M.; Ostarcevic, E.; Li, J.-D.; Gray, S. Identification of material and physical features of membrane distillation membranes for high performance desalination. *J. Membr. Sci.* **2010**, *349*, 295–303. [\[CrossRef\]](#)
39. Shirazi MM, A.; Kargari, A.; Tabatabaei, M. Evaluation of commercial PTFE membranes in desalination by direct contact membrane distillation. *Chem. Eng. Process. Process Intensif.* **2014**, *76*, 16–25. [\[CrossRef\]](#)
40. Boubakri, A.; Hafiane, A.; Bouguecha, S.A.T. Application of response surface methodology for modeling and optimization of membrane distillation desalination process. *J. Ind. Eng. Chem.* **2014**, *20*, 3163–3169. [\[CrossRef\]](#)
41. Gunko, S.; Verbych, S.; Bryk, M.; Hilal, N. Concentration of apple juice using direct contact membrane distillation. *Desalination* **2006**, *190*, 117–124. [\[CrossRef\]](#)
42. Heloisa, R.; Francisco, M.R.A.; Cintia, M.; Ramlow, H.; Machado, R.A.F.; Marangoni, C. Direct contact membrane distillation for textile wastewater treatment: A state of the art review. *Water Sci. Technol.* **2017**, *76*, 2565–2579.
43. Ni, W.; Li, Y.; Zhao, J.; Zhang, G.; Du, X.; Dong, Y. Simulation study on direct contact membrane distillation modules for high-concentration NaCl solution. *Membranes* **2020**, *10*, 179. [\[CrossRef\]](#) [\[PubMed\]](#)
44. Ali, E. Novel structures of direct contact membrane distillation for brackish water desalination using distributed feed flow. *Desalination* **2022**, *540*, 116000. [\[CrossRef\]](#)
45. Chen, T.C.; Ho, C.D.; Yeh, H.M. Theoretical modeling and experimental analysis of direct contact membrane distillation. *J. Membr. Sci.* **2009**, *330*, 279–287. [\[CrossRef\]](#)
46. Banat, F.A.; Simandl, J. Desalination by membrane distillation: A parametric study. *Sep. Sci. Technol.* **1998**, *33*, 201–226. [\[CrossRef\]](#)
47. Manawi, Y.M.; Khraisheh, M.A.M.M.; Fard, A.K.; Benyahia, F.; Adham, S. A predictive model for the assessment of the temperature polarization effect in direct contact membrane distillation desalination of high salinity feed. *Desalination* **2014**, *341*, 38–49. [\[CrossRef\]](#)
48. Su, M.; Teoh, M.M.; Wang, K.Y.; Su, J.; Chung, T.-S. Effect of inner-layer thermal conductivity on flux enhancement of dual-layer hollow fiber membranes in direct contact membrane distillation. *J. Membr. Sci.* **2010**, *364*, 278–289. [\[CrossRef\]](#)
49. Hayer, H.; Bakhtiari, O.; Mohammadi, T. Simulation of momentum, heat and mass transfer in direct contact membrane distillation: A computational fluid dynamics approach. *J. Ind. Eng. Chem.* **2015**, *21*, 1379–1382. [\[CrossRef\]](#)
50. Venault, A.; Chang, K.Y.; Maggay, I.V.; Chang, Y. Assessment of the DCMD performances of poly (vinylidene difluoride) vapor-induced phase separation membranes with adjusted wettability via formation process parameter manipulation. *Desalination* **2023**, *560*, 116682. [\[CrossRef\]](#)
51. Yang, G.; Ng, D.; Huang, Z.; Zhang, J.; Gray, S.; Xie, Z. Janus hollow fibre membranes with intrusion anchored structure for robust desalination and leachate treatment in direct contact membrane distillation. *Desalination* **2023**, *551*, 116423. [\[CrossRef\]](#)
52. Tian, M.; Yuan, S.; Decaesstecker, F.; Zhu, J.; Volodine, A.; Van der Bruggen, B. One-step fabrication of isotropic poly (vinylidene fluoride) membranes for direct contact membrane distillation (DCMD). *Desalination* **2020**, *477*, 114265. [\[CrossRef\]](#)
53. Zhang, J.; Gray, S.; Li, J. Modelling heat and mass transfers in DCMD using compressible membranes. *J. Membr. Sci.* **2012**, *387–388*, 7–16. [\[CrossRef\]](#)

Disclaimer/Publisher’s Note: The statements, opinions and data contained in all publications are solely those of the individual author(s) and contributor(s) and not of MDPI and/or the editor(s). MDPI and/or the editor(s) disclaim responsibility for any injury to people or property resulting from any ideas, methods, instructions or products referred to in the content.